Short Sisal Fiber Reinforced Styrene–Butadiene Rubber Composites

R. PRASANTHA KUMAR,[1] M. L. GEETHAKUMARI AMMA,[2] and SABU THOMAS[1,*]

[1]School of Chemical Sciences, Mahatma Gandhi University, Priyadarshini Hills P.O., Kottayam-686 560, Kerala, India, and [2]Rubber Research Institute of India, Ministry of Commerce, RRII P.O., Kottayam-686 009, Kerala, India

SYNOPSIS

Styrene–butadiene rubber (SBR) composites were prepared by incorporating short sisal fibers of different lengths and concentrations into the SBR matrix in a mixing mill according to a base formulation. The curing characteristics of the mixes were studied and the samples were vulcanized at 150°C. The properties of the vulcanizates such as stress–strain behavior, tensile strength, modulus, shore-A hardness, and resilience were studied. Both the cured and uncured properties showed a remarkable anisotropy. It has been found that aspect ratio in the range of 20–60 is effective for sufficient reinforcement. The mechanical properties were found to increase along and across the grain direction with the addition of fibers. The effects of fiber length, orientation, loading, type of bonding agent, and fiber–matrix interaction on the properties of the composites were evaluated. The extent of fiber orientation was estimated from green strength measurements. The adhesion between the fiber and the rubber was enhanced by the addition of a dry bonding system consisting of resorcinol and hexamethylene tetramine. The bonding agent provided shorter curing time and enhanced mechanical properties. The tensile fracture surfaces of the samples have been examined by scanning electron microscopy (SEM) to analyze the fiber surface morphology, orientation, fiber pull-out, and fiber–matrix interfacial adhesion. Finally, anisotropic swelling studies were carried out to analyze the fiber–matrix interaction and fiber orientation. © 1995 John Wiley & Sons, Inc.

INTRODUCTION

Short fibers are used in rubber compounding due to the considerable processing advantages, improvement in certain mechanical properties, and for economic considerations.[1] Both natural and synthetic fibers can be incorporated into the rubber matrix along with other additives. The composites thus prepared can be used for extrusion, calendering, and various types of molding operations such as compression, injection, and transfer. The addition of suitable short fiber improves or modifies the properties of the composite.

The short fiber composites have been studied by several researchers in an attempt to fabricate reinforced products like V-belts,[2] hoses,[3] tyre treads,[4] and complex shaped articles.[5]

When used properly, short fibers generate a high degree of reinforcement which is sufficient for many specific applications. The efficiency of a composite can be increased by the preservation of high aspect ratio of the fiber, control of fiber directionality, generation of a strong interface through physico-chemical bonding, and establishment of high degree of dispersion.[6] An aspect ratio of 100–200 is generally required for effective reinforcement in short fiber elastomer composites.[7] During milling operations, the majority of fibers tend to orient along the flow direction to cause good orientation. The parameters which must be considered most important in affecting short fiber reinforcement are fiber aspect ratio, the type of fiber, type of matrix, fiber length, fiber orientation, fiber concentration, fiber dispersion, and the adhesion between the fiber and matrix.[8] The reinforcement of an elastomer with short fibers

combines the elasticity of the rubber matrix with strength and stiffness of the fibers.[9]

O'Connor[10] has studied the effect of short synthetic fibers in rubber compounds. Short glass fibers were used for reinforcing rubbers due to their high modulus, high strength, and low creep.[11] The mechanical properties of carbon, polyester, glass, polyamide, and cellulose in ethylene propylene diene monomer (EPDM), natural rubber (NR), chloroprene rubber (CR), nitrile rubber (NBR) and styrene–butadiene rubber (SBR) matrices have been studied by Ibarra et al.[12,13] Coran et al.[14] have investigated the effect of various fibers such as glass, rayon, nylon, and cellulose in both natural rubber and synthetic rubber matrices.

The widely used inorganic fillers, such as glass and mica, are very expensive compared to natural fibers. Nowadays, studies have been conducted on how to conserve energy from renewable resources. Natural fibers are important due to the renewable nature, low cost, easy availability, and easiness for chemical and mechanical modifications. They are also free of the health hazards so frequently associated with the use of synthetic fibers. Moreover, it is evident from the ratio of cost to load carried by the fiber that natural fibers are a highly cost effective form of reinforcement.[15] Lignocellulosic fibers such as jute, sisal, coir, pineapple, bamboo, hemp, bagasse, flax, cotton, banana, and straw have been used as reinforcements in different matrices.[16] Among these fibers, jute is extensively used for reinforcement in NR and carboxylated nitrile rubber (XNBR) matrices.[17,18] The effects of bonding agent and alkali treatment on the mechanical properties of coir-fiber-reinforced NR composites have been studied by Arumugam[19] and Geethamma et al.[20] Setua and Dutta[21] have studied the effect of bonding agent in short silk-fiber-reinforced polychloroprene rubber composites. The morphological and mechanical properties of oriented cellulose-fiber-reinforced elastomeric composites have been studied by Coran and co-workers.[22] The mechanical properties of the short jute-fiber-reinforced SBR composites have also been studied by Murty and De.[23]

The fracture surfaces of the composites have been studied by several researchers in order to observe the fiber orientation, fiber pull-out and fiber–matrix interaction. Murty[24] has carried out studies on the failure surfaces of short glass fiber rubber composites by scanning electron microscopy. Recently, in this laboratory, Thomas and co-workers have extensively studied the physico-mechanical properties on short sisal, coir, and pineapple leaf fiber (PALF) rein-

forced low-density polyethylene (LDPE),[25,26] polystyrene (PS)[27] and NR[20,28] composites.

Styrene–butadiene rubber (SBR) is a general-purpose synthetic rubber which finds extensive applications for the manufacture of various rubber products. However, the material exhibits poor mechanical properties due to its amorphous and nonstrain crystalline nature.

Over the years, various fillers, have been used for the reinforcement of SBR. However, no serious attempt has been made so far to evaluate the use of short sisal fiber as a reinforcing filler for SBR matrix. In this study, we have evaluated the effect of fiber length, fiber distribution, fiber orientation, fiber concentration, and bonding agent on the physical and mechanical properties of short sisal-fiber-reinforced SBR composites. Fiber–matrix adhesion has been analyzed by scanning electron microscopy studies and anisotropic swelling measurements.

EXPERIMENTAL

Sisal fiber, which is extensively grown in the southern parts of India, is supplied by a local processing unit situated in the state of Tamil Nadu. It was reported that sisal fibers contain 78% cellulose, 10% hemicellulose and pectins, 8% lignin, 2% waxes, and 1% ashes.[29] The physical properties of the sisal fiber are given in Table I. The raw sisal fibers were chopped to different lengths viz., 2, 6, 10 mm and washed with water to remove the undesirable materials. Then these fibers were dried in an air oven at 70°C for 5 h, and it was then kept in polythene bags to prevent moisture absorption.

Styrene–butadiene rubber (SBR-1502) used for the present study was the technically specified form of the rubber, and the same lot was used for the entire experiment. The bonding agents hexamethylene tetramine and resorcinol used for the experiment were of laboratory reagent grade. All other ingredients incorporated into the SBR matrix were of commercial grade. The recipe used for the present work is shown in Tables II and III.

Table I Physical Properties of Sisal Fiber

Physical Property	Sisal Fiber
Density (g/cm³)	1.45
Diameter (μm)	100–300
Elongation at break (%)	4–9
Tensile strength (MPa)	450–700
Young's modulus (MPa)	7,000–13,000

Table II   Formulation of Mixes A to D

Ingredients	Mixes			
	A	B	C	D
SBR-1502[a]	100	100	100	100
Sulfur	2.2	2.2	2.2	2.2
Stearic acid	2	2	2	2
Zinc oxide	5	5	5	5
CBS[b]	1	1	1	1
TDQ[c]	1	1	1	1
Sisal fiber				
(Untreated)	—	35	35	35
)er length, mm)	—	(2)	(6)	(10)

[a] SBR with bound styrene content, 21.5–25.5%; obtained from Synthetics and Chemicals Bareilly, U.P., India, |ML(1 + 4)| at 100°C, 46–58; volatile matter 0.75%; organic acid 4.75–7%; soap 0.5%; ash 1.5%; antioxidant 0.5–1.5%.

[b] N-cyclohexyl benzothiazyl sulfenamide.

[c] 2,2,4-Trimethyl 1,2-dihydro quinoline polymerized.

Mixes were prepared by means of a laboratory two-roll open-mixing mill (150 × 300 mm). The nip gap, mill-roll speed ratio (1 : 1.25), time and temperature of mixing, number of passes, and sequence of addition of ingredients during mixing were kept the same for all mixes. The chopped fibers were added to the SBR matrix at the end of the compounding process without any chemical treatment. The rolling direction was kept always the same to promote better fiber orientation.

Mill shrinkage of the compound was determined b   itting a piece of a compounded sheet from the open mill as per ASTM standard D 1917-89. Green strength was determined by using a method developed by Foldi.[30] The strength of uncured 2-mm-thick samples were measured at a strain rate of 50 cm min⁻¹. The surface tack was eliminated by pressing the sample at 120°C for 2 min between two sheets of aluminum film in a hydraulic press.

Shear forces occurring during milling operations orient most of the fibers along the grain direction, but this also caused fiber breakage. In order to study the extent of fiber breakage, the fibers were extracted from the green compound by dissolving the rubber compound in toluene, and their length and diameter were measured by using a traveling microscope.

The curing characteristics were studied by an oscillating disk rheometer (Monsanto rheometer R-100). The samples were vulcanized at 150°C in a hydraulic press having electrically heated platens to their respective cure times as obtained from the rheographs. Stress–strain measurements were carried out by using a Universal Testing Machine

(ZWICK-1474) at a crosshead speed of 50 cm min⁻¹. Tensile measurements of the composites were determined using samples cut along (longitudinally oriented fiber) and across (transversely oriented fiber) the grain direction. Modulus, tensile strength, and elongation at break were determined according to ASTM method D 412-68. Figure 1 shows the longitudinal and transverse fiber orientation.

Resilience was determined at 28°C using a Dunlop tripsometer according to BS 903 part-2, 1950. Hardness was measured at room temperature by using a shore-A hardness tester (Durometer) ASTM D-2240-81 test method. Resilience and hardness measurements were made with tensile sheets without considering the orientation of fibers.

Anisotropic swelling studies were carried out using rectangular samples cut at different angles with respect to orientation of the fiber from the tensile sheets and swollen in toluene at room temperature for 3 days. The tensile failure surfaces (Fig. 1) were examined by scanning electron microscopy (SEM). The fracture surfaces were sputter-coated with gold within 24 h of testing by using a fine coat JFC-1100. SEM studies were carried out using a JEOL scanning electron microscope model JSM 35C.

RESULTS AND DISCUSSION

Fiber Breakage

Due to the high shear forces caused during mixing, fibers usually undergo breakage, and their breakage pattern can be indicated by fiber length distribution curve. The distribution of fiber lengths can be represented in terms of moments of the distribution.[31,32]

The number- and weight-average fiber lengths can be defined as

$$\bar{L}_n = \frac{\sum N_i L_i}{\sum N_i} \tag{1}$$

$$\bar{L}_w = \frac{\sum N_i L_i^2}{\sum N_i L_i} \tag{2}$$

where $\bar{L}_n$ is the number-average fiber length, $\bar{L}_w$ the weight-average fiber length, and N_i the number of fibers having length L_i.

The value of $\bar{L}_w/\bar{L}_n$, the polydispersity index, can be taken as a measure of fiber length distribution. The values of L_n, L_w and L_w/L_n are calculated based on 100 fibers for the chopped sisal fibers and fibers extracted from the mix. Table IV shows the fiber

Table III Formulation of Mixes E to L

Ingredients	Mixes							
	E	F	G	H	I	J	K	L
SBR-1502	100	100	100	100	100	100	100	100
Sulfur	2.2	2.2	2.2	2.2	2.2	2.2	2.2	2.2
Stearic acid	2	2	2	2	2	2	2	2
Zinc oxide	5	5	5	5	5	5	5	5
Resorcinol	—	—	—	—	—	—	—	5
Hexa[a]	---	----	---	---	—	---	...	2.5
CBS[b]	1	1	1	1	1	1	1	1
TDQ[c]	1	1	1	1	1	1	1	1
Sisal fiber								
(Untreated)	5	10	15	20	15	20	25	35
(Fiber length, mm)	(6)	(6)	(6)	(6)	(10)	(10)	(10)	(6)

[a] Hexamethylene tetramine.
[b] N-cyclohexyl benzothiazyl sulfenamide.
[c] 2,2,4-Trimethyl 1,2-dihydro quinoline polymerized.

length distribution index of untreated sisal fibers before and after the mixing. The value of $\bar{L}_w/\bar{L}_n$ remains about the same before and after processing, indicating that no considerable fiber breakage occurred during mixing.

Figure 2 shows the fiber length distribution curve of untreated sisal fibers before and after mixing. After mixing, the majority of fibers are distributed between 5 and 6 mm. It was observed that the majority

of fibers had an aspect ratio of 20–60 after mixing. In the case of jute fiber rubber composites, the aspect ratio of 40 was reported to be sufficient for reinforcing rubber matrix, since there was very good adhesion between the fiber and rubber.[33] Since sisal is a lignocellulosic fiber, it bends and curls during milling due to its intrinsic flexible nature. Therefore, the breakage of sisal fiber was low when it was used as reinforcement in SBR matrix. Hence the initial
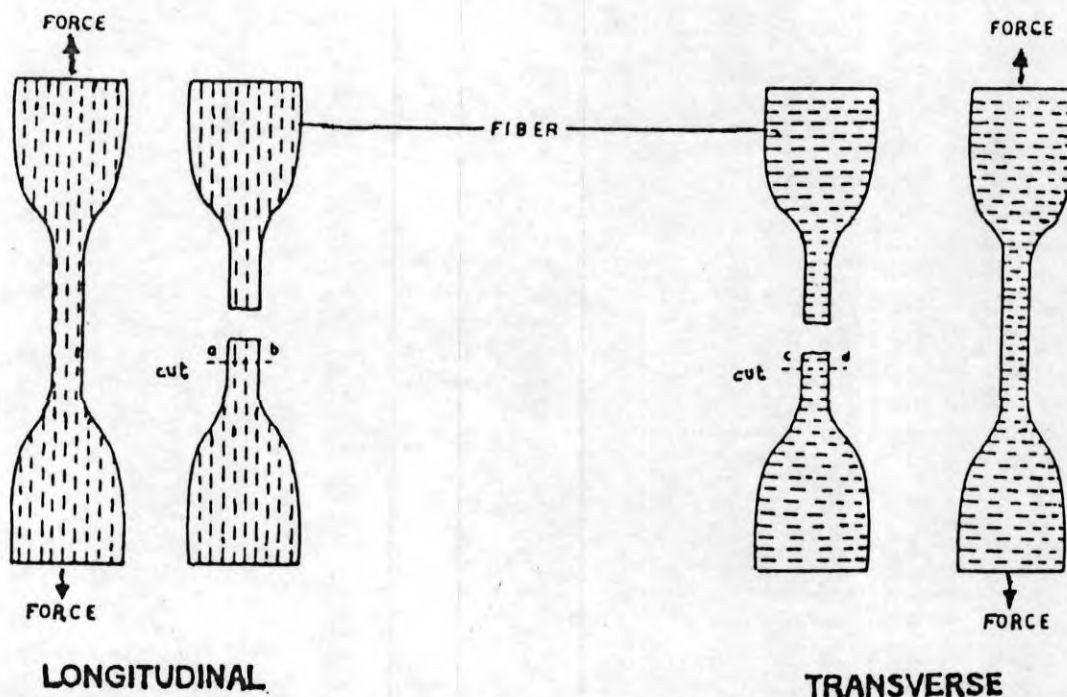

Figure 1 Tensile samples with fiber orientation and corresponding fractured surfaces.

Table IV   Fiber Length Distribution Index

Sisal fiber	$\bar{L}_n$ (mm)	$\bar{L}_w$ (mm)	$\bar{L}_w/\bar{L}_n$
Before mixing	5.9	5.98	1.014
After mixing	4.63	5.06	1.093

aspect ratio (before mixing) of around 20–60 is preserved in the composites. On the other hand, synthetic fibers like glass, carbon, and so forth undergo severe breakage during mixing.[32] The average diameter (0.1212 mm) of the sisal fiber remained the same after mixing.

Effect of Fiber Length

Curing Characteristics

The curing behavior of various mixes are given in the Figure 3. In general, for all mixes the torque initially decreases, then increases and finally levels off. The initial decrease in torque to a minimum value is due to the softening of the rubber matrix. The increase in the torque is due to the crosslinking of the rubber. The leveling off is an indication of the completion of curing. It is found that the addition of fibers increases the torque value of the SBR compound. It can be seen that the torque value increases with an increase in fiber length. This increase in the torque of the system is due to the presence of longer fibers which impart more restriction to deformation. However, maximum torque was slightly higher for 6 mm than for 10 mm length. The curves in the rheographs cross over each other because of their differences in cure times. It is reported that the increase in torque is directly proportional to the crosslink density.[34] The Table V shows the effect of fiber length on the cure time and scorch time of mixes A, B, C, and D. It can be seen that as the fiber length decreases, the scorch time and cure time decreases. This is due to the fact that at the same loading as the fiber length decreases, the number of ends increases. The increased fiber ends generate more heat due to friction.[20]

Mechanical Properties

The properties of short fiber-reinforced elastomer composites depend on the degree to which an applied load is transmitted to the fibers. This extent of load transmittance is a function of fiber length and magnitude of fiber–matrix interaction. At a critical fiber length, the load transmittance from the matrix to fiber is maximum. If critical fiber length (l_c) is greater

than the length of the fiber, the stressed fiber will debond from the matrix and the composite will fail at low load. If l_c is less than the length of the fiber, the stressed composites will lead to breaking of fibers. The critical fiber length for different fiber composites have been determined by Thomas and co-workers. The l_c for coir fiber–NR, sisal fiber–LDPE, PALF–LDPE, sisal fiber–PS, and sisal fiber–NR composites were 10, 6, 6, 6, and 10 mm, respectively.[20,25-28]

The stress–strain curves of mixes A (gum), B, C, and D are shown in Figure 4. The deformation behavior of the blends can be understood from the stress–strain curve. Addition of fiber increase the modulus of the compound. The increase is quite high in the case of longitudinally oriented composites. The longitudinally oriented composites show brittle-type behavior while transversely oriented composites show elastic deformation. In both directions fiber lengths of 6 mm showed the maximum tensile strength and modulus. However, the elongation at break reduced with the increase in fiber length.

Table VI shows the effect of fiber length on tensile strength, elongation at break, hardness, and tensile
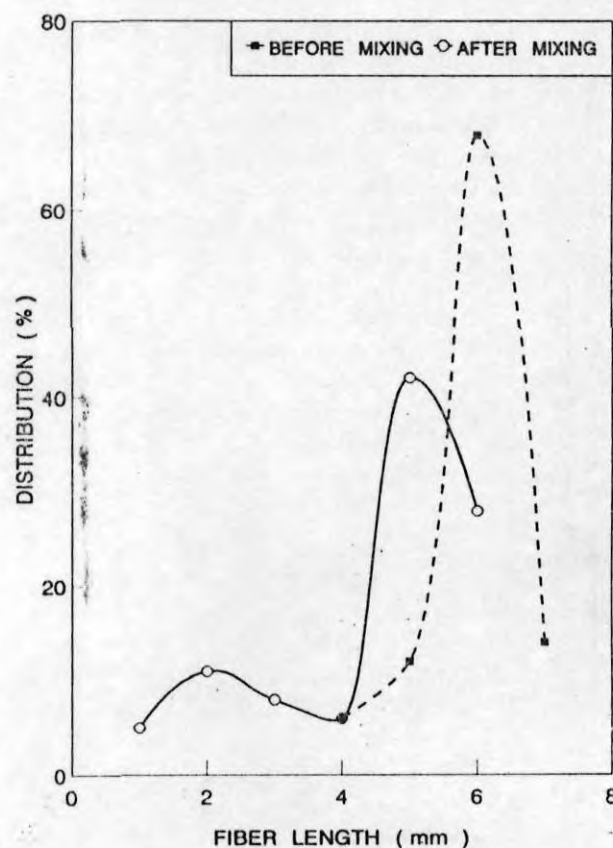

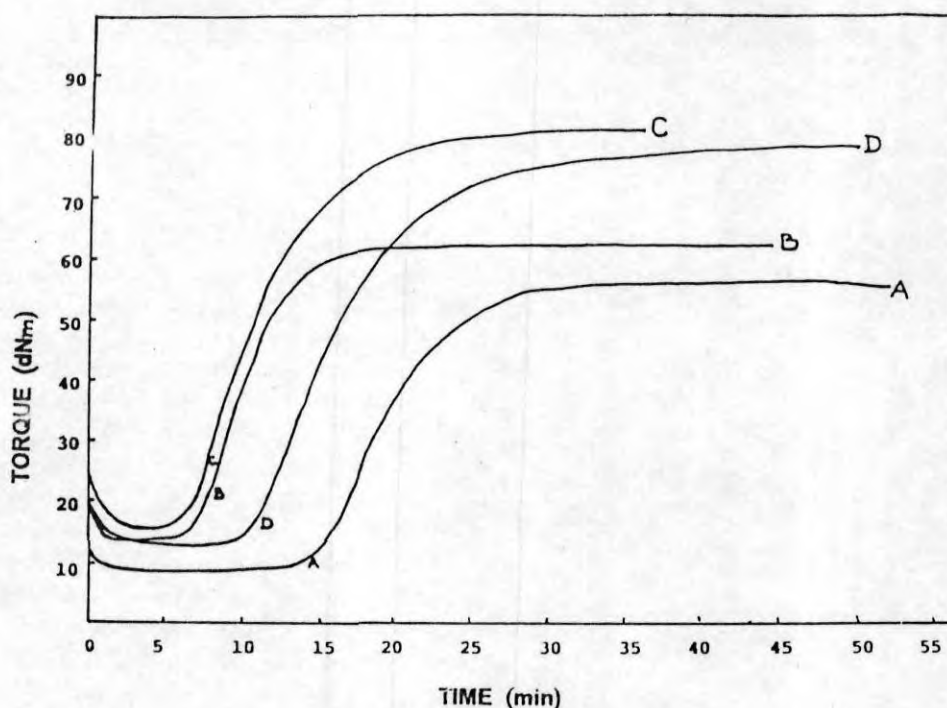Figure 2   Fiber length distribution curve of fibers before and after mixing.

Figure 3   Rheographs of mixes A, B, C, and D.

moduli at different elongations and orientations. The moduli at 10 and 20% elongations showed a maximum value for composite containing sisal fiber of length 6 mm and then decreased at a length of 10 mm. This trend has been found at both orientations. The tensile strength of the composites also showed a maximum value at 6 mm fiber length. The increase in fiber length beyond 6 mm marginally reduces the strength of the composite.

The interfacial interaction between rubber matrix and fiber reaches a maximum value when the fiber length is 6 mm and the effect of fiber length disappears with longer fibers because of fiber entanglement and breakage. At higher fiber lengths, the dispersion of fibers in the rubber matrix becomes very difficult. To achieve better dispersion of fibers, repeated passing through the mill rolls is necessary. This will cause the entanglement and breakage of long fibers.

From the overall mechanical property studies, it is found that the critical fiber length of 6 mm is effective for reinforcement in SBR matrix.

Fiber Orientation

Fiber orientation affects the performance of composite properties.[35] For example, the balanced fiber orientation in a hose gives optimum design strength.[36] For a fixed mill opening, all the possible fiber orientation will be achieved during the first pass. But a poorly dispersed fiber composite requires more than one pass to achieve dispersion in addition to fiber orientation. The properties of milled short fiber elastomer composites depend only on mill opening and not on mill-roll speed, roll speed ratio, or number of passes.[37] The complete orientation of fibers in a given direction is practically impossible. However, depending on the fiber type, loading, and rubber matrix, it is possible to orient the majority of fibers.

During milling of rubber composites, the fibers tend to orient along the flow direction, causing mechanical properties to vary in different directions.[38] The optimum properties of the composites can be obtained by controlling the flow direction. A large shear flow during milling forces fibers to orient along the mill direction.

Extent of Fiber Orientation

The extent of fiber orientation can be understood qualitatively from the examination of the fracture surfaces of the samples by SEM photographs. Figure 5(a) shows the tensile failure surface of longitudinally oriented composite (mix C). The broken fiber ends protruding from the fracture surface indicate that the fibers are well aligned longitudinally in the direction of the applied force. Figure 5(b) shows

fracture surfaces of the transversely oriented composites (mix C). Here, the fibers are aligned across the direction of the applied force.

Table VII shows the green strength and orientation values of the various mixes. From the difference in green strength in machine direction (longitudinal direction) and across machine direction (transverse direction), the extent of orientation can be calculated by using the following equation:[34]

$$\text{Orientation (\%)} = \frac{S_L/S_{G,L}}{S_L/S_{G,L} + S_T/S_{G,L}} \quad (3)$$

where S denotes the green strength of the composite and subscripts L, T, and G denote longitudinal, transverse, and gum compounds, respectively. Although the extent of fiber orientation is maximum in mix G, mixes H, C, and L also show high extent of fiber orientation (Table VII). The fiber orientation is lowest in mix E.

Effect of Orientation on Mechanical Properties

When the fibers are aligned longitudinally, the maximum stress transfer occurs between the fiber and matrix. The maximum strength and reinforcement are achieved along the direction of fiber alignment. Reinforcement is virtually nonexistent in the transverse direction because the fibers act as barriers that prevent the distribution of stresses throughout the matrix.

The mechanical properties such as tensile moduli and tensile strength are found to be higher in the longitudinal direction than in the transverse direction (Table VI). SEM studies revealed that fiber-filled composites exhibit a marked change in fracture topography [Figs. 5(a) and (b) and 6(a)]. The pres-
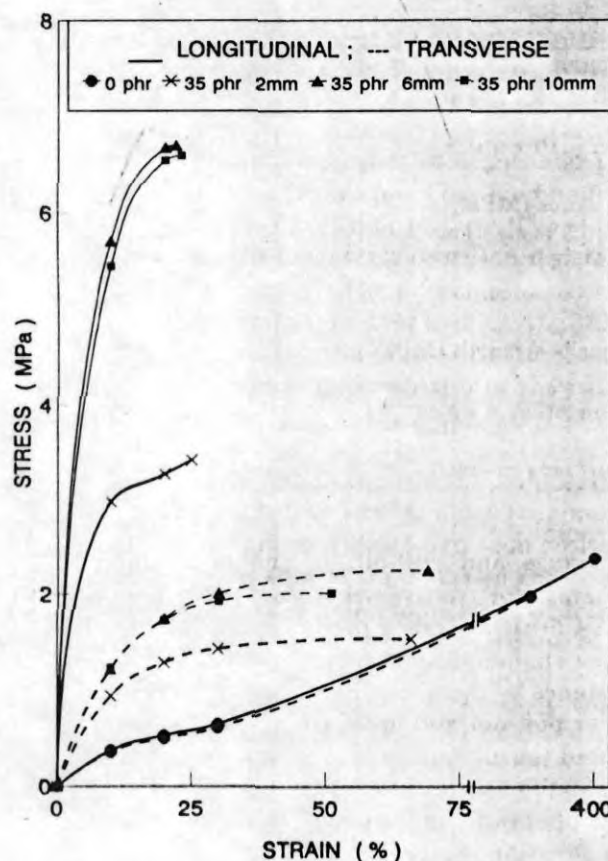

Figure 4 Stress–strain curves of mixes A, B, C, and D.

ence of fibers in the mix altogether changes the failure modes. The fracture of fiber-reinforced composites occurs in two modes[39]: (i) breakage of fiber leading to failure and (ii) pull-out of several fibers from the matrix. In the case of longitudinally oriented fiber composites [Fig. 5(a)], the fibers are oriented perpendicular to the fracture front. Hence

Table V Vulcanization Characteristics of Mixes A to L

Mixes	T_{max} (dNm)	T_{min} (dNm)	ΔT (dNm)	t_{90} (min)	Scorch time (min)
A	56.0	8.9	47.1	29.15	14.0
B	61.0	13.0	48.0	14.0	6.5
C	81.0	16.10	64.9	17.15	6.25
D	70.5	11.25	59.25	18.15	10.0
E	71.0	8.8	62.2	19.0	7.0
F	72.0	11.0	61.0	17.5	6.5
G	75.0	11.0	64.0	18.0	7.0
H	76.0	11.7	64.3	17.1	7.15
I	70.5	11.0	59.5	25.25	10.5
J	78.0	11.25	66.75	22.35	9.0
K	75.0	13.0	62.0	25.25	10.25
L	97.0	19.5	77.5	6.05	1.0

Table VI   Effect of Fiber Length on Properties of Mixes

Properties	Orientation	Mixes			
		A	B	C	D
Modulus (MPa)					
10% elongation	L	0.37	3.25	6.03	5.40
	T	0.36	0.96	1.22	1.18
20% elongation	L	0.53	3.64	6.66	6.55
	T	0.50	1.13	1.75	1.64
Tensile strength (MPa)	L	2.36	3.75	6.70	6.60
	T	2.07	1.56	2.24	1.99
Elongation at break (%)	L	400	25	23	21
	T	288	70	69	65
Hardness Shore-A		43	70	80	81

breakage and pull-out of the fibers take place, whereas for transversely oriented fiber composites [Fig. 5(b)] the crack progresses in the direction of fiber alignment, experiencing, therefore, a lower resistance by the fibers. Figures 6(a) and (b) show the fiber pull-out and breakage in a longitudinally oriented tensile failure sample (mix C). In the longitudinally oriented tensile failure sample of mix C, the fiber pull-out is very prominent due to the lack of adhesion between fiber and rubber matrix.

Effect of Fiber Loading

Curing Characteristics

Figure 7 shows the rheograph of mixes A, C, E, F, G, and H. The presence of fibers generate an increase in viscosity in the mixes. The increase in the torque value from the minimum value (M_L) to the maximum value (M_H) as measured from the rheographs indicate the increase in the stiffness of the fiber-reinforced materials. Mix A requires a longer vulcanization time as it is the conventional vulcanization system without any fiber. The increase in fiber loading from 5 to 35 phr in the mixes has no considerable effect on the cure time and scorch time (Table V).

Mechanical Properties

The presence of short fibers increases the green strength of the compound. Table VII shows that green strength increases with the increase in concentration of fibers. In the longitudinal orientation, green strength of the compound increases rapidly up to 10 volume percent of loading followed by a leveling off at higher loading. In transverse direction, it shows only a marginal increase. In both orienta-

tions, green strength shows its maximum value at 35 phr loading (mix C).

The stress–strain response to various fiber loadings is shown in Figure 8. It can be seen that the deformation behavior of the composites are different. The addition of fiber results in an increase in modulus and reduction in elongation at break at both orientations. The maximum properties are seen in the case of composites having a loading of 35 phr. The stress–strain curves of longitudinally oriented composites at high fiber loading (35 phr) show brittle-type behavior. However, transversely oriented composites show ductile-type behavior.

The effect of fiber loading on the tensile moduli at different elongations in both orientations of the composites is shown in Table VIII. Modulus shows a continuous increase up to 17.7% volume loading of fiber in the case of longitudinal orientation. On transverse orientation, the modulus increases gradually.

The reinforcement of polymers with short fibers usually leads to an increase in tensile strength of amorphous rubbers.[40] The effect of fiber loading on tensile strength of sisal–SBR composites in both directions is shown in Table VIII. The behavior is typical of the amorphous rubbers. The tensile strength in the longitudinal direction increases with increase in fiber concentration. However, there is a slight decrease at 5% volume loading. On further increase in loading, tensile strength continuously increases. This is due to the fact that at low fiber concentration the fiber acts as a flaw in the rubber matrix. At low fiber loading the matrix is not restrained by enough fibers, and highly localized strains occur in the matrix at low stresses, causing the bond between the fiber and rubber to break leaving the matrix diluted by nonreinforcing debonded
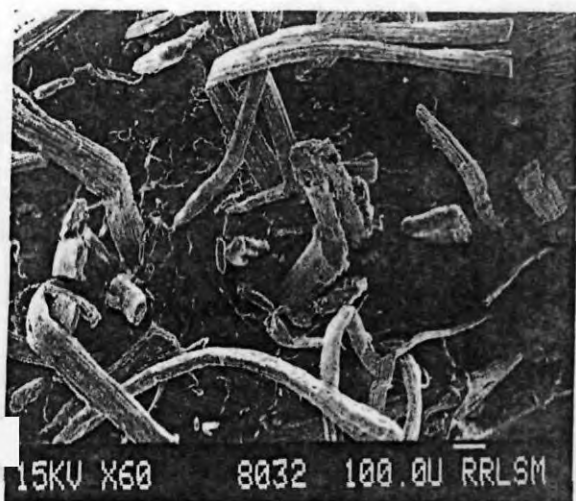
a
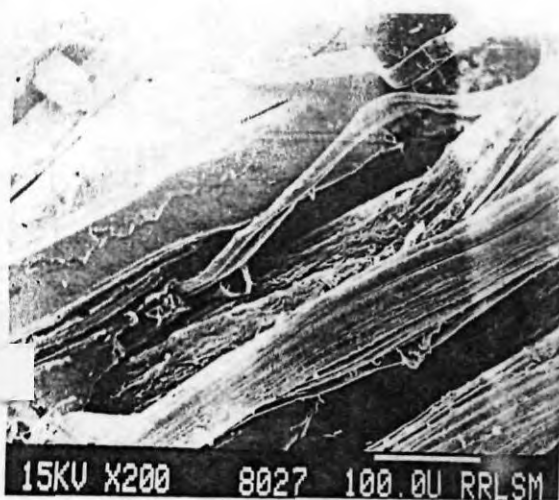
b

Figure 5 (a) SEM photograph showing longitudinal orientation of fibers in SBR composite (mix C). (b) SEM photograph showing transverse orientation of fibers in untreated SBR composite (mix C).

fibers. As the fiber concentration increases from 5 to 35 phr, the stress is more evenly distributed and the strength of the composite increases. Many workers reported a detailed study on the anisotropy in mechanical properties.[34,38,41] It is important to mention that our study was limited to 17.7% volume loading of fiber. This is due to the fact that above this loading, the incorporation of fibers into SBR matrix was difficult due to the entanglement of fibers during the mixing operations. This results in the

breakage of fibers in the mixes. In the case of transverse orientation, no improvement in tensile strength was observed upon the addition of fibers.

Table VIII shows the elongation at break of mixes as a function of fiber loading. It indicates a sharp fall in elongation at break at low fiber loading followed by a leveling off at higher loading. The elongation at break in the transverse direction registers higher values as compared to longitudinally oriented composites. With increase in fiber loading, the stiffness and brittleness of the composite increased gradually with an associated decrease in the elongation at break.

The incorporation of sisal fibers into the SBR matrix increases the hardness of the composite. Hardness is related to the strength and toughness of the short fiber-reinforced elastomeric composites. Due to the close packing of the fibers in the composite, the density is also found to increase with the addition of fibers. Resilience decreases with increase in fiber loading. Table VIII shows the decrease in resilience and increase in hardness property with the increase in concentration of sisal fibers in SBR matrix.

Effect of Bonding Agent

Curing Behavior

The addition of bonding agent, resorcinol-hexa system, showed a considerable effect on the curing behavior of the SBR compounds. On analyzing Figure 9, it is seen that the bonding agent containing mix L showed a shorter cure time than mix C. The difference in the maximum and minimum torque values $(M_H - M_L)$ points toward a greater crosslinking density for mix L. This is due to the fact that the adhesion between the fiber and matrix is improved due to the greater interaction between the lignocellulosic sisal fiber and SBR matrix through the

Table VII   Green Strength and Orientation

Mixes	Green Strength (MPa)		Orientation (%)
	Longitudinal	Transverse	
A	0.29	0.24	—
E	0.39	0.35	49.25
F	0.61	0.35	59.45
G	0.91	0.36	68.07
H	0.93	0.38	67.60
C	1.02	0.49	64.03
L	1.21	0.56	64.92

bonding agent. The addition of bonding agent reduces the optimum cure time and scorch time (Table V). The decrease in scorch time values indicates the reduction in scorch safety of the compound containing bonding agent. It was also noted that rate of vulcanization is faster in mix L than in mix C.

Mechanical Properties

Figure 10 shows the stress–strain curves for the unbonded system (mix C) and bonded system (mix L) at 35 phr loading. Compared to other mixes, mix *L* containing bonding agent showed superior mechanical properties. The resorcinol-hexa system enhances the interaction between fiber and the SBR matrix. Tensile strength, modulus at 10 and 20% elongations, and hardness were found to change favorably with the addition of bonding agent into the untreated fibers (Table IX). This is due to the increase in adhesion between the rubber and fiber through bonding agent. The high level of fiber–rubber adhesion causes breakage of the fibers without pulling them out of the rubber matrix in the longitudinal direction. However, no improvement could be seen in the transverse direction (Fig. 12).

The Figures 11 and 12 show the SEM of tensile failure surfaces of longitudinally and transversely oriented composites of mix L containing 35 phr sisal fiber and bonding agent. The failure surface of the longitudinally oriented composite (Fig. 11) shows features of well-developed interfacial interaction. Clearly, there are very low pull-out of fibers on the fracture surface. On comparing the fracture surfaces of bonded and unbonded tensile failure surfaces of longitudinally oriented composites [Figs. 6(a) and 11], it is seen that there are very low pull-out of fibers on the fracture surface of bonded ones. This indicates better adhesion due to the presence of bonding agent in mix L. The fiber breakage and pull out become insignificant in the transversely oriented composites as shown in Figure 12. However, since the fibers are oriented transversely, the properties do not show any improvement.

Anisotropic Swelling Studies

Swelling is a uniform restrictive force induced on the vulcanizate samples. Because of the anisotropic nature of the fiber–rubber composites, swelling is restricted in the direction of fiber alignment and consequently the swelling becomes anisotropic. Sisal fibers exhibit higher anisotropy, particularly at higher fiber loadings in the presence of bonding agent. But at low fiber loadings, the anisotropy is
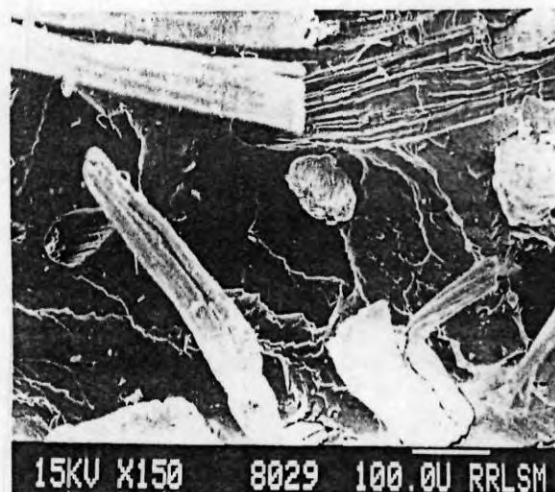
a
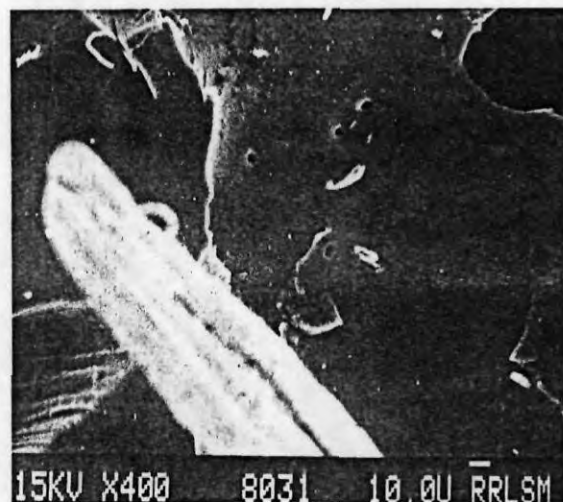
b

Figure 6 (a) SEM photograph showing fiber breakage and holes developed due to pull-out of fibers (mix C). (b) Magnified version of SEM photograph showing fiber breakage and holes developed due to pull-out of fibers (mix C).

not considerable, especially in the case of the untreated fiber composites. This is possibly due to the poor bonding between sisal fiber and SBR matrix.

Das[42] has studied the swelling behavior of short fiber-reinforced elastomeric composites. Recently, in our laboratory, Varghese et al. studied the swelling behavior of NR composites in various aromatic solvents.[43] These studies provided information on the strength of interface, degree of dis-
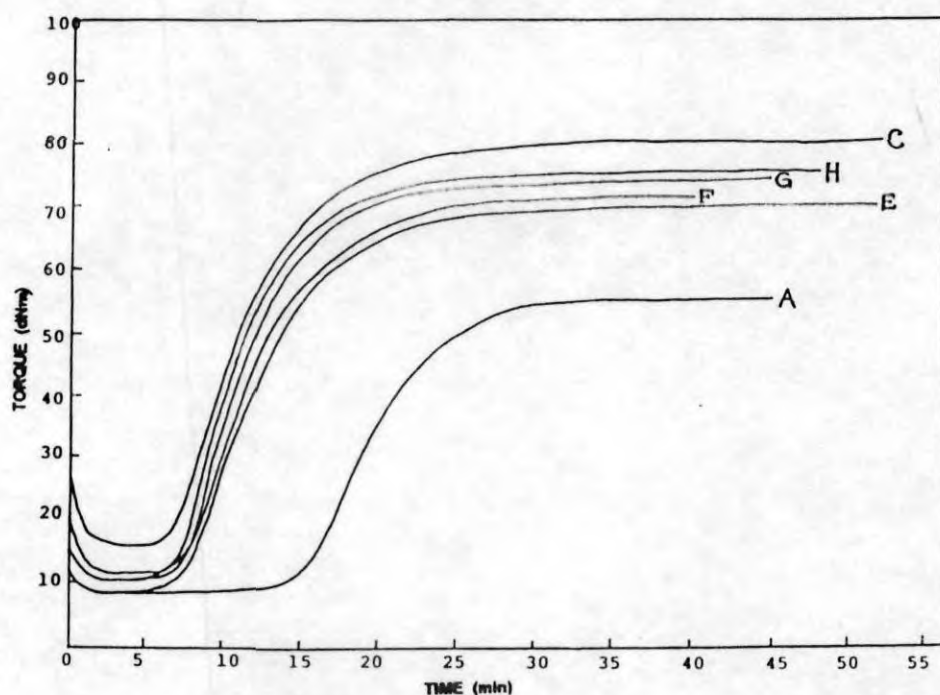
Figure 7   Rheographs of mixes A, C, E, F, G, and H.

person of fibers, and their alignment in the elastomeric matrix.

The swelling behavior of composites can be analyzed from the swelling coefficient values as calculated by the following equation:[44]

$$\text{Swelling coefficient } (\alpha) = \frac{M_\infty - M_0}{M_0} \times d1 \quad (4)$$

where M_∞ denotes the weight of the solvent at the equilibrium swelling, M_0 the initial weight of the sample, and d the density of the solvent. Table X shows the swelling coefficients of the composites containing different fiber loadings and bonding agent. As the loading of fiber increases, the values of the swelling coefficient decreases. It indicates that the solvent uptake behavior of the composites reduces at higher loading of fibers. The minimum swelling coefficient values of mix L show better adhesion between sisal fiber and SBR. The bonding agent present in the composite binds the fiber and rubber so that swelling is highly restricted in the composite.

The volume fraction, V_r, of SBR in the specimen swollen in toluene was determined after 72 h at room temperature using the following equation[45] to establish the extent of crosslinking:
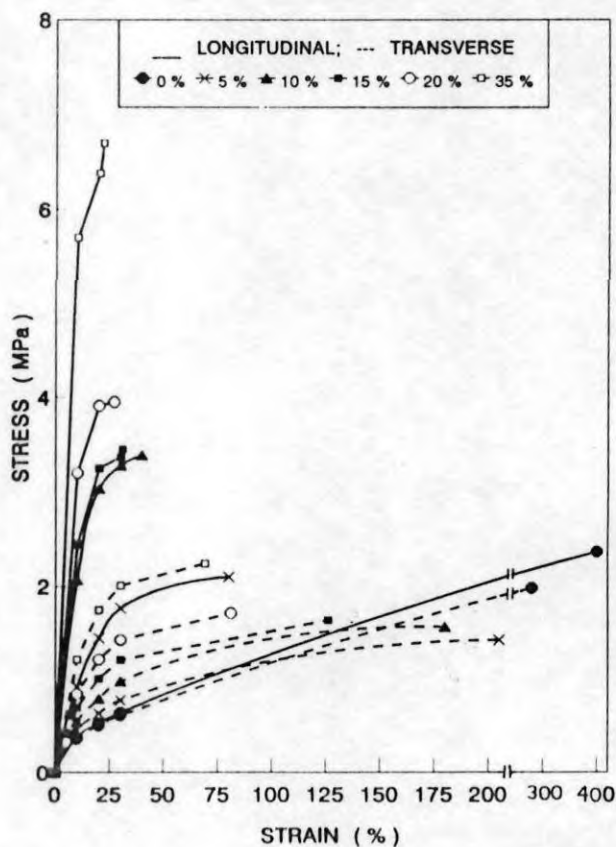

Figure 8   Stress strain curves of mixes A, C, E, F, G, and H in transverse and longitudinal directions.

Table VIII   Effect of Fiber Loading on Properties of Mixes

Properties	Orientation[a]	Mixes					
		A	E	F	G	H	C
Modulus (MPa)	L	0.37	0.93	2.07	2.45	3.20	6.03
10% elongation							
	T	0.36	0.45	0.54	0.70	0.85	1.22
20% elongation	L	0.53	1.45	3.03	3.25	3.91	6.66
	T	0.50	0.64	0.79	1.02	1.42	1.75
Tensile strength (MPa)	L	2.36	2.10	3.39	3.45	3.95	6.70
	T	2.07	1.43	1.56	1.64	1.72	2.24
Elongation at break (%)	L	400	80	40	30	27	23
	T	288	221	180	126	81	69
Hardness Shore-A		43	46	57	63	71	80
Resilience (%)		76.10	66.73	65.55	64.59	63.58	61.52

[a] L, longitudinal; T, transverse.

$$V_r = \frac{(D - fT)\rho_r^{-1}}{(D - fT)\rho_r^{-1} + A_0\rho_s^{-1}} \quad (5)$$

where D is the weight after drying out, f the fraction of insoluble components, T the weight of the sample, ρ_r the density of rubber (SBR = 0.94 g/cm³), ρ_s the density of solvent (toluene = 0.866 g/cm³), and A_0 the weight of the imbibed solvent. Table XI shows volume fraction of rubber, V_r, in various mixes. The

higher V_r value for mix L signifies greater fiber-rubber interaction.

A comparison of crosslink density has been made from the reciprocal swelling values, $1/Q$, where Q is defined as grams of the solvent per gram of the hydrocarbon, which is calculated[18] by

$$Q = \frac{\text{Solvent swollen wt.} - \text{Dried wt.}}{\text{Original wt.} \times 100/\text{Formula wt.}} \quad (6)$$
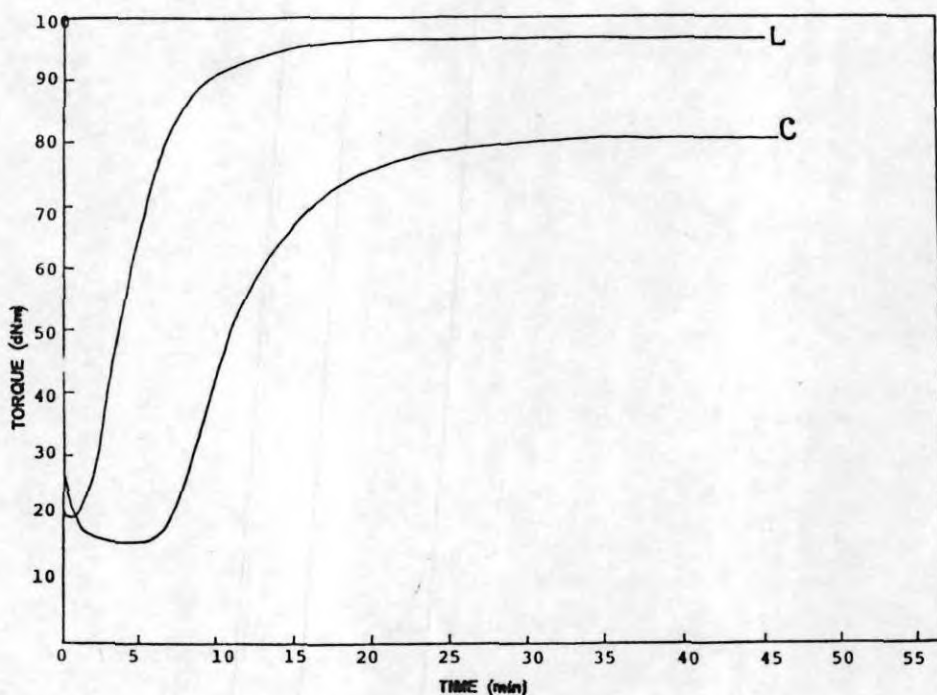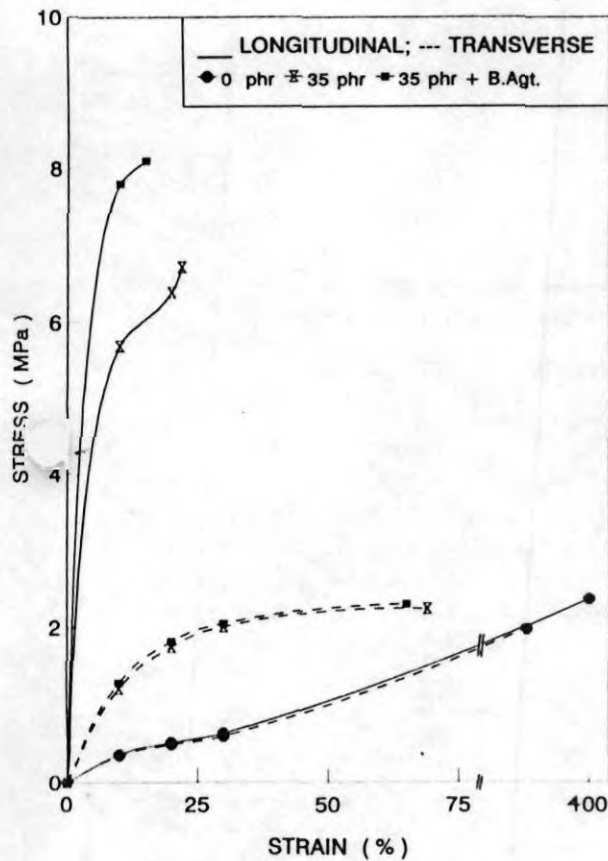

Figure 9   Rheographs of mixes C and L.

Figure 10 Stress–strain curves of bonded and unbonded mixes.

Figure 11 SEM photograph showing better adhesion between fiber and matrix in longitudinally oriented composite containing bonding agent (mix L).

Table XI shows the effect of bonding agent on apparent crosslinking values in various mixes. Mix L shows maximum crosslink density. It indicates maximum interaction between the fiber and matrix.

Figure 13 is the representation of a unidirectional composite specimen before (solid line) and after (dotted line) swelling. The length of the line l_0 taken at an angle θ with the fiber direction grows during

swelling to a length l_s; a_L is taken in the direction of fiber orientation, OY (lengthwise), a_T is taken in the OX direction (breadthwise), while a_Z value is taken in the OZ direction (widthwise).

If $X_s/X_0 = a_T$, $Y_s/Y_0 = a_L$, and $l_s/l_0 = a_\theta$, then the swelling ratio a_θ in any direction forming an angle θ with fiber orientation is given by the following expression:[46]

$$a_\theta^2 = (a_T^2 - a_L^2)\sin^2\theta + a_L^2 \qquad (7)$$

where a_L and a_T are the dimensional swelling variations with an angle θ between measurement direction and fiber orientation.

Swelling in the transverse direction of fibers is greater than that in longitudinal direction. Hence a_T values are greater than a_L as indicated in the Table XII. The difference between the a_T and a_Z values

Table IX   Mechanical Properties of Mixes

Mixes	Orientation[a]	Modulus (MPa) Elongation 10%	20%	Tensile Strength (MPa)	Elongation at Break (%)	Hardness Shore-A	Resilience (%)
A	L	0.37	0.53	2.36	373	43	76.10
	T	0.36	0.5	2.07	288		
C	L	5.7	6.38	6.70	23	80	61.52
	T	1.22	1.75	2.24	69		
L	L	7.8	—	8.10	15	86	58.26
	T	1.29	1.82	2.30	65		

[a] L, longitudinal; T, transverse.

Figure 12 SEM photograph showing better adhesion between fiber and matrix on transverse orientation.

implies that the orientation of fibers is not perfectly unidirectional, which arise due to the flow produced during molding.

Samples wherein θ was 0 or 90° remained rectangular after swelling. Figure 14 shows the relationship between swelling-induced linear deformation and fiber orientation for mixes A, C, and L. The plots of a_θ^2 against $\sin^2 \theta$ for these mixes are found to be straight lines having slope $a_T^2 - a_L^2$ and intercept a_L^2. It is seen that a_θ values increase with θ values. It indicates a preferential fiber orientation in the grain direction.

The extent of fiber alignment can be understood from the slope values given in Table XII. Noguchi et al.[47] have reported that the steeper the line the higher the degree of fiber alignment. Mix L shows the maximum slope value among the various mixes. It shows that the bonding agent added composites that have better fiber alignment.

Table X Swelling Coefficient

Mixes	Weight of Sample (g)	Weight of Solvent Imbibed (g)	Swelling Coefficient
A	0.4232	1.6240	4.4320
E	0.4212	1.4036	3.8480
F	0.4358	1.4550	3.8562
G	0.4414	1.5123	3.9570
H	0.4609	1.4139	3.5430
C	0.4736	1.3862	3.3806
L	0.5327	0.8066	1.7480

Table XI Effect of Bonding Agent on Volume Fraction (V_r) and Crosslinking ($1/Q$)

Mixes	Apparent Crosslinking ($1/Q$)	Volume Fraction of Rubber (V_r)
A	0.23	0.18
C	0.23	0.18
L	0.41	0.28

Moreover, swelling studies help us to comment about the interface bonding. Mix L shows the lowest a_L and a_T values, and the line corresponding to mix L in Figure 14 shows the highest slope. This indicates that a good interface bonding has occurred between the fiber and matrix in mix L.

CONCLUSION

The mechanical properties of short sisal-fiber-reinforced SBR composite have been analyzed as a function of fiber length, orientation, loading, and bonding agent. Fiber length of 6 mm was found to be optimum for the best balance of properties. Composites containing longitudinally oriented fibers show superior mechanical performance than that of
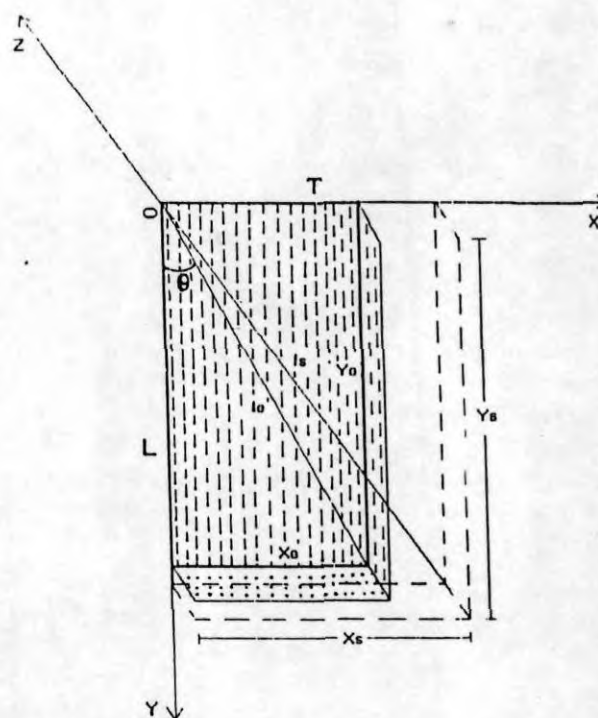

Figure 13 Geometry of the swelling of unidirectional composite.

the transverse orientation. The addition of short sisal fibers to SBR offers good reinforcement and causes improvement in mechanical properties which further gets strengthened by the presence of bonding agent. At 35 phr loading of sisal fiber, composite showed maximum properties, and mechanical anisotropy is observed at this loading.

The adhesion between the fiber and rubber can be enhanced by the use of resorcinol-hexa bonding system. The improvement in interfacial interaction between fiber and SBR was substantiated by means of SEM studies. From green strength measurements, the extent of fiber orientation was analyzed and f   l that mix G has better fiber orientation than other mixes due to the better dispersion of fibers during mixing. The extent of fiber alignment and the adhesion between the untreated fiber and SBR matrix with and without bonding agent have been evaluated by swelling measurements.

Table XII   Anisotropic Swelling

Mixes	a_L	a_T	a_Z	Slopes
A	1.70	1.75	1.50	0.1608
C	1.67	1.69	1.50	0.9476
L	1.04	1.50	1.95	1.1955

Figure 14 Relationship between swelling-induced linear deformation and fiber orientation.

REFERENCES

1. D. C. Derringer, *Rubber World*, **45**, 165 (1971).
2. J. W. Rogers, *Rubber World*, **27**, 183 (1981).
3. L. A. Goettler, A. J. Lambright, R. I. Leib, and P. J. Dimauro, *Rubber Chem. Technol.*, **54**, 274 (1981).
4. J. R. Beatty and P. Hamed, *Elastomerics*, **27**, 110 (1978).
5. Technical Report No. 34, Rubber Chemicals Div., Monsanto Co., Louvian La Neuve, Belgium (1983).
6. R. L. Ibarra, A. C. Chamorro, and R. M. C. Tabernero, *Polym. Compos.*, **9**(3), 198 (1988).
7. S. Varghese, B. Kuriakose, S. Thomas, and A. T. Koshy, *Ind. J. Nat. Rubber Res.*, **4**(1), 55 (1991).
8. P. Hamed and A. Y. Coran, *Additives Plast.*, **1**, 29 (1978).
9. D. C. Derringer, *J. Elastoplastics*, **3**, 230 (1971).
10. J. E. O'Connor, *Rubber Chem. Technol.*, **50**, 945 (1977).
11. J. Campbell, *Prog. Rubber Technol.*, **41**, 43 (1976).
12. L. Ibarra, *J. Appl. Polym. Sci.*, **49**, 1595 (1993).
13. L. Ibarra and C. Chamorro, *J. Appl. Polym. Sci.*, **37**, 1197 (1989).
14. A. Y. Coran, K. Boustany, and P. Hamed, *Rubber Chem. Technol.*, **47**, 396 (1974).
15. R. S. P. Coutts, Anzaas, Search, **19**(4), 195 (1988).
16. Y. S. Zuev, T. Karpovich, and M. F. Bukhina, *Kauch Rezina*, **28**(6) (1978).
17. D. K. Setua and S. K. De, *Rubber Chem. Technol.*, **56**, 808 (1983).
18. S. K. Chakraborty, D. K. Setua, and S. K. De, *Rubber Chem. Technol.*, **55**, 1286 (1982).
19. N. Arumugam, K. Tamaraselvy, K. Venkata Rao, and P. Rajalingam, *J. Appl. Polym. Sci.*, **37**, 2645 (1989).
20. V. G. Geethamma, R. Joseph, and S. Thomas, *J. Appl. Polym. Sci.*, **55**, 583 (1995).
21. D. K. Setua and B. Dutta, *J. Appl. Polym. Sci.*, **29**, 3097 (1984).
22. A. Y. Koran, P. Hamed, and L. A. Goettler, *Rubber Chem. Technol.*, **49**, 1167 (1976).
23. V. M. Murty and S. K. De, *J. Appl. Polym. Sci.*, **29**, 1355 (1984).
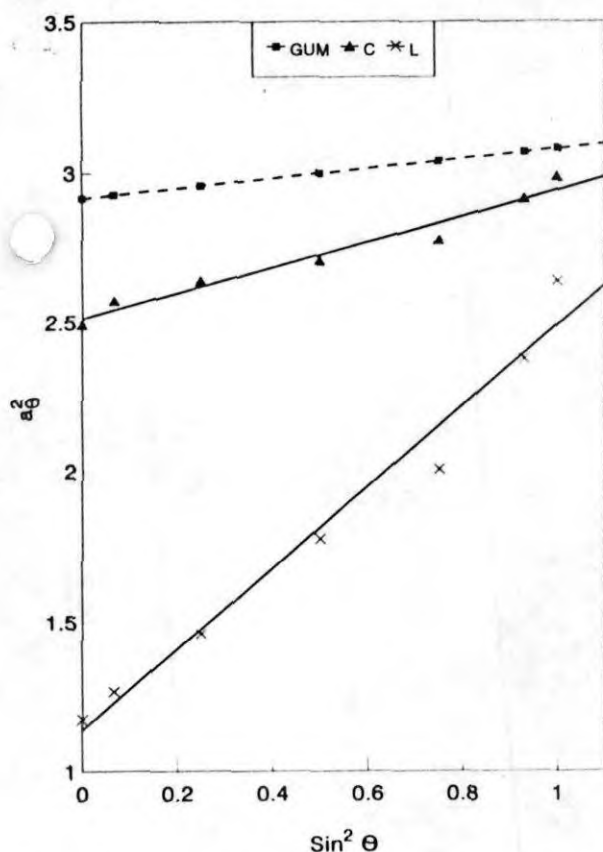24. V. M. Murty, *Intern. J. Polymeric Mater.*, **10**, 149 (1983).

25. K. Joseph, C. Pavithran, and S. Thomas, *J. Appl. Polym. Sci.*, **47**, 1731 (1993).
26. J. George, S. S. Bhagawan, N. Prabhakaran, and S. Thomas, *J. Appl. Polym. Sci.*, to appear.
27. K. C. Manikandan Nair, S. M. Diwan, and S. Thomas, *J. Appl. Polym. Sci.*, to appear.
28. S. Varghese, B. Kuriakose, S. Thomas, and A. T. Koshy, *J. Adhesion Sci. Technol.*, **8**(3), 235 (1994).
29. B. C. Barkakatty, *J. Appl. Polym. Sci.*, **20**, 2921 (1976).
30. A. P. Foldi, *Rubber Chem. Technol.*, **49**, 379 (1976).
31. H. Morawetz, *Macromolecules in Solution*, 2nd ed., Interscience, New York, 1975.
32. L. Czarnekei and J. L. White, *J. Appl. Polym. Sci.*, **25**, 1217 (1980).
33. V. M. Murty and S. K. De, *Rubber Chem. Technol.*, **55**, 287 (1982).
34. L. Ibarra and C. Jorda, *J. Appl. Polym. Sci.*, **48**, 375 (1993).
35. J. E. Ashton, J. C. Halpin, and P. H. Petit, *Primer on Composite Materials*, Technomic Publication Co., West Fort, CT, 1969.
36. Goettler (to Monsanto), German, 46068 W 28 DT 2461-183 (Aug. 1975).
37. S. R. Moghe, *Rubber Chem. Technol.*, **49**, 1160 (1976).
38. A. Y. Coran, K. Boustany, and P. Hamed, *J. Appl. Polym. Sci.*, **15**, 2471 (1971).
39. V. M. Murty, A. K. Bhowmick, and S. K. De, *J. Mater. Sci.*, **17**, 709 (1982).
40. L. Broutman and R. Krock, *Modern Composition Materials*, Moscow, 'Mir' Publishers, 1970 (Russian translation).
41. L. A. Goettler and K. S. Shen, *Rubber Chem. Technol.*, **56**, 619 (1983).
42. B. Das, *J. Appl. Polym. Sci.*, **17**, 1019 (1973).
43. S. Varghese, B. Kuriakose, S. Thomas, and K. Joseph, *Rubber Chem. Technol.*, to appear.
44. U. S. Aithal and T. M. Aminabhavi, *J. Chem. Edn.*, **67**(1), 82 (1990).
45. S. Thomas, B. Kuriakose, B. R. Gupta, and S. K. De, *Plast. Rubber Proce. Appl.*, **6**, 101 (1986).
46. L. Ibarra and C. Chamorro, *J. Appl. Polym. Sci.*, **43**, 1805 (1991).
47. T. Noguchi, M. Ashida, and S. Mashimo, *Nippon Gomu Kyokaishi*, **57**(3), 171 (1984).